Agricultural Water Management 285 (2023) 108370

Contents lists available at ScienceDirect

Agricultural Water Management

journal homepage: www.elsevier.com/locate/agwat

Quantifying water productivity and nitrogen uptake of maize under water and nitrogen stress in arid Northwest China

Junjun Ran [a], Hui Ran [a,*], Longfei Ma [a], Stewart A. Jennings [b], Tinggao Yu [a], Xin Deng [a], Ning Yao [a], Xiaotao Hu [a]

[a] Key Laboratory of Agricultural Soil and Water Engineering in Arid and Semiarid Areas, Ministry of Education, Northwest A & F University, Yangling, Shaanxi 712100, China

[b] Institute for Climate and Atmospheric Science, School of Earth and Environment, University of Leeds, Leeds LS2 9JT, UK

ARTICLE INFO

Handling Editor Dr Z Xiying

Keywords:
Plant water relationship
Nitrogen dilution curve
Nitrogen use efficiency
Stress
Water productivity model
Nitrogen uptake model

ABSTRACT

Water and nitrogen (N) are critical determinants of crop water productivity (WP) and N uptake (N_{uptake}), and are also key factors in crop modelling. Through a two-year field experiment with three irrigation levels (full irrigation (W1), moderate water stress (W0.75), and severe water stress (W0.5)), three N application rates (150, 75, and 0 kg N ha^{-1}, i.e., N150, N75, and N0) and three replications for each treatment in Northwest China, we quantified the effects of water and N stress on the growth, yield, and water and N use efficiency (WP and NUE) of hybrid seed maize (*Zea mays L.* cv. Tianruifeng). Furthermore, nonlinear dynamic water productivity (WP) models and water (ET)-based N_{uptake} models were developed. The results showed that water stress had a larger impact than N stress on the growth and yield of maize, with water stress reducing yield (Y), final aboveground biomass (B), and N uptake by 36.5%, 15.4%, and 25.7% on average, respectively, and N stress decreasing them by 18.7%, 12.3%, and 13.6%, respectively. Biomass-based water productivity ($WP_{B\text{-}ET}$) and yield-based water productivity ($WP_{Y\text{-}ET}$) at the end of the growth period responded differently to water stress but similarly to N stress because of a higher decrease of harvest index (HI) under water stress than under N stress. Specifically, $WP_{Y\text{-}ET}$ decreased significantly while $WP_{B\text{-}ET}$ kept relatively stable as water stress increased. The variation of the measured WP during the growth period presented a single peak trend. The Logistic, Sigmoid, and Linear models showed similar high accuracy for quantifying the relationship between evapotranspiration accumulation and biomass growth. However, the derived WP values from the nonlinear dynamic models were more in line with the single peak variation of the measured WP during the growth period, with the agreement index (d) improved from 0.21 to 0.65–0.75 in comparison to the Linear model. The developed ET-based N accumulation models can quantify N uptake through evapotranspiration. The results can contribute to improving the accuracy of crop modelling under drought stress conditions, and the design of irrigation and N management in arid and semi-arid regions.

1. Introduction

The area of water-saving irrigation in China has increased from 27.3 million ha to 37.8 million ha from 2010 to 2020, while agricultural fertilizer application decreased to 51.9 million tons in 2021 after reaching a peak of 60.2 million tons in 2015, with nitrogen (N) fertilizer application declining from 24.0 million tons to 18.3 million tons from 2012 to 2020 (National Data, 2022). Reducing the consumption of water and N resources is needed for the future sustainable development of agriculture in arid and semi-arid regions under the context of climate change, because of limited water and damaging environmental impacts of excess N (Zhang et al., 2015; Kang et al., 2017). Therefore, research on the response of crop growth and resource use efficiency to water and N stress and its simulation in models is necessary for informing optimal water and N management strategies, synergistically improving yields and water and N use efficiencies, and promoting sustainable agricultural development and ensuring food security in these regions.

Water productivity (WP) is a key indicator to investigate water management and sustainable development of agriculture in arid and semi-arid regions. Current studies on WP include comprehensive

* Corresponding author.
E-mail addresses: ranhui1990@126.com, huiran@nwsuaf.edu.cn (H. Ran).

https://doi.org/10.1016/j.agwat.2023.108370
Received 6 December 2022; Received in revised form 27 April 2023; Accepted 12 May 2023
Available online 22 May 2023

evaluation of the final WP at the end of the growth season (Ran et al., 2017; El-Sanatawy et al., 2021; Kang et al., 2021; Lu et al., 2022), and investigation of the dynamic processes of WP during the growth period (Steduto et al., 2007; Ran et al., 2019). Several studies have reported that water stress during the whole growth period significantly decreases yield-based water productivity ($WP_{Y\text{-}ET}$) (Wang et al., 2019; Ye et al., 2022). However, biomass-based water productivity ($WP_{B\text{-}ET}$) of maize responded insignificantly to water stress under 100–500 kg N ha^{-1} N application conditions (Ran et al., 2017). N application usually increases both $WP_{Y\text{-}ET}$ and $WP_{B\text{-}ET}$ (Ran et al., 2017; Li et al., 2019; Guo et al., 2022; Zhang et al., 2022). In addition, the variation of the final $WP_{Y\text{-}ET}$ is highly related to the time, duration, and extent of water stress. For example, Kang et al. (2000) revealed that maize yield responds insignificantly to water stress at the seedling stage, resulting in an increase in $WP_{Y\text{-}ET}$. A comparison of the responses of $WP_{Y\text{-}ET}$ and $WP_{B\text{-}ET}$ to water and N stress is lacking. Ran et al. (2017) found a difference in the response of $WP_{Y\text{-}ET}$ and $WP_{B\text{-}ET}$ to water stress at relatively high N application levels, without fully taking into account zero N application conditions. On the other hand, WP is normally considered as a constant during the growth period (Steduto et al., 2007; Tsegay et al., 2011; Adeboye et al., 2017). However, Hsiao et al. (2009) observed a law of increasing, then stabilizing and finally decreasing WP along the maize growth period by fitting the relationship between measured biomass and evapotranspiration accumulation. Ran et al. (2019) further quantified the dynamic process of WP using Logistic and Sigmoid models and improved the accuracy of crop modelling under non-stress conditions in comparison to a fixed WP. Logistic and Sigmoid models have the advantage of capturing the "S" shape characteristics of biomass accumulation versus transpiration in comparison to Linear models, and WP derived from the Logistic and Sigmoid models is a bell curve instead of a constant (Ran et al., 2019). However, the nonlinear dynamic WP model developed by Ran et al. (2019) did not consider N stress. Therefore, it is necessary to further investigate the response of final $WP_{Y\text{-}ET}$ and $WP_{B\text{-}ET}$ at the end of the crop growth season to water and N stress, as well as the dynamic change of WP to water and N stress and its modelling during the crop growth period.

Nitrogen use efficiency (NUE) is typically evaluated to determine the capability of crop uptake of N fertilizer from the soil. Many studies demonstrated that N application can increase the effectiveness and accessibility of soil available N (Ashraf et al., 2016), promote crop N assimilation (Santachiara et al., 2018), maintain the grain filling process and yield formation in the reproductive growth stage (Li et al., 2022a,b; Liu et al., 2022), and enhance N harvest index (NHI) and N seed production efficiency (NUE_g) (Che et al., 2015). However, extra N application does not show a significant advantage on maize biomass accumulation nor on yield, rather reduced N recovery efficiency (RE_N) and yield-based N use efficiency (NUE_{yield}) (Wang et al., 2019; Ye et al., 2022), resulting in an increased N mineralization rate (Tarkalson et al., 2022). Recent studies have further identified significant correlations between soil water status and N uptake (Qiang et al., 2022; Wang et al., 2022; Zhang et al., 2022), and found that water stress inhibits maize N uptake and utilization (Guo et al., 2022; Jégo et al., 2022). Tarkalson et al. (2022) showed that overwatering decreases NUE and yield. However, current studies mainly qualitatively analyze the relationship between water status and N uptake, and quantitative models are lacking. Therefore, there is a need to further investigate the quantitative relationship between N uptake and water status (ET) of maize at each growth stage, and provide a simple way to diagnose the N nutrient status of crops through crop water conditions.

In this study, we hypothesize that WP responds differently to water and N stress, and N accumulation can be quantified through evapotranspiration. To address the above issues, we conducted a two-year field experiment with nine irrigation and N treatments each year in arid Northwest China to quantify the influence of water and N stress on the growth and resource use efficiencies of maize and develop corresponding process-based dynamic models. The objectives of this study were to (1) explore the response of final WP and NUE to water and N stress; (2) improve nonlinear dynamic WP models by accounting for stress conditions; (3) develop an ET-based N uptake model, so as to support water saving and N reduction strategies in arid Northwest China.

2. Materials and methods

2.1. Experimental site and its description

The experiment was conducted at the National Scientific Field Observation and Research Station for Efficient Water Use in Oasis Agriculture in Wuwei, Gansu Province (102°50′E, 37°52′N, elevation 1581 m) in 2018 and 2019. The region has a typical temperate continental arid climate with an average annual precipitation of 164 mm, average annual temperature of 8 ℃, and total annual accumulated temperature of 3550 ℃ d (Yuan et al., 2019; Liao et al., 2022). The soil is silty loam with an average bulk density of 1.4 g cm^{-3} for 0–100 cm soil layers, field capacity of 0.3 cm^3 cm^{-3}, and wilting coefficient of 0.1 cm^3 cm^{-3} (Ran et al., 2018).

2.2. Experimental methods

In this experiment, the variety of hybrid seed maize was *Tianruifeng.* A complete 2 × 3 factorial design was used, which had two factors (water and nitrogen), each with three levels. Three independent replications were taken at each of the 9 (3^2) treatment combinations, resulting in a total of 27 (3^2 ×3) experimental plots. The layout of the plots followed a randomized complete block design. The three irrigation levels were full irrigation (W1), moderate deficit irrigation (W0.75), and severe deficit irrigation (W0.5), and the three N-fertilization rates consisted of applications of 150 (N150), 75 (N75), and 0 kg N ha^{-1} (N0) (see supplementary material, Table S1). Irrigation was controlled according to the actual soil water content of the W1N150 treatment. In order to ensure that no water stress occurred during the growth period of the W1N150 treatment, the soil water content in the root zone was maintained at no less than 65% of the field capacity (Ran et al., 2017). The soil water content for each of the three plots of the W1N150 treatment was monitored with an interval of 10–15 days during the non-intensive evapotranspiration period and an interval of 5–7 days during the intensive water consumption period. Irrigation was applied when the soil water depletion touched the lower threshold of 65% of the field capacity. The irrigation amount for the W1 level was calculated based on the difference between actual soil water content and the upper threshold of field capacity. The irrigation depth of the W0.75 and W0.5 levels was 75% and 50% of the W1 irrigation depth, respectively. The same irrigation depth was applied to ensure the emergence of maize in all experimental plots each year (Table S1). The application of N fertilizer was divided into base N and top dressing N with a 1:1 ratio. The base N was applied 5 cm below the soil surface before planting, and the top dressing was applied through irrigation during the jointing stage of the female plants.

Maize was sowed on 15 April and harvested in mid-September in 2018 and 2019. It was planted with five rows of female plants and one row of male plants. The plant spacing was 0.25 m and row spacing was 0.4 m, with a planting density of 100,000 plants ha^{-1}. The experimental plot area was 24 m^2, and each plot was separated by ridges with a width of 0.4 m and a height of 0.3 m. Bulk rows were planted between the plots to avoid the edge effect on crop growth and resource use. The irrigation method was border irrigation on plots fully covered with perforated plastic mulch. The N, phosphate, and potassium fertilizer were urea (N ≥ 46%), phosphorus pentoxide (P_2O_5 ≥ 16%), and potassium oxide (K_2O ≥ 51%), respectively. The field management of weeding, disease and pest control, and phosphate and potassium fertilizer application is consistent with local agricultural production.

2.3. Measurements

Meteorological data were collected every 15 min using the weather station (Hobo, Onset Computer Crop., USA) located at the experimental site. Measurements included solar radiation, air temperature, wind speed at 2 m aboveground, relative humidity, and precipitation. Daily precipitation and temperature during the maize growth period are shown in Fig. S1.

During the maize growth period, aboveground biomass was sampled every 10–15 days. Three whole plants were randomly selected and cut off from the ground for each treatment each time, and all plants sampled were manually divided into leaves (including all green and dead leaves), stems (including all stems and leaf sheaths), and ears (including all husks, cobs, and kernels), separately. They were firstly dried at 105 °C for 30 min to deactivate enzyme activity, then dried to constant weight at 70 °C and weighed. The mean value of the three sampled plants from repeated plots is taken as the aboveground biomass of the corresponding treatment. At the end of the growth period, all plants in a 1 m^2 square area in the center of each plot were cut to measure final biomass and yield. Each plant was manually divided into three parts of stem, leaf, and ear, and the ear was subdivided into husk, cob, and kernel. The drying method and the way for calculating the mean value for each treatment were the same as the time series plant samples. The yield was converted from the oven drying weight of the kernel to the weight with a water content of 13% for comparison between different treatments.

Soil water content was measured using the oven drying method every 10–15 days. Three sampling sites were taken for each treatment from the three corresponding replicated plots. Each sampling site was set at the center of four adjacent plants in two rows. Soil samples were collected at 0–10 cm, 10–20 cm, 20–40 cm, 40–60 cm, 60–80 cm, and 80–100 cm depths using a stainless-steel soil auger. The auger holes were refilled with the surrounding soil after each sampling to avoid significant preferential flow during irrigation and heavy rainfall. Soil samples were dried to constant weight in an oven at 105 °C for 8 h. Volumetric water content was obtained by multiplying gravimetric content by bulk density. The weighted average soil water content of each soil layer was then calculated for each replication. The mean value of the three sampling sites represented the soil water content of the corresponding treatment.

Plant N concentration and accumulation were measured after each biomass measurement. All the divided and dried plants from each plot were separately ground and passed through a 0.5 mm sieve, resulting in three sets of sieved dry matter powder for each part of the plants for each treatment. Three equal amounts of 0.5 g samples, randomly taken from the three sets of powder for each plant part, were used to measure the N concentration for each treatment using the Kjeldahl method (Miao et al., 2022) during the growth period. N uptake in the aboveground part was obtained by summing the product of the N concentration of each part and the corresponding biomass weight. The mean value of the three replications was taken as the plant N concentration and uptake of the corresponding treatment.

Evapotranspiration (ET) was calculated using the water balance method, with the reference formula in Liao et al. (2022). Time series WP along the growth period was computed as the ratio of the difference in two adjacent samples of biomass (ΔB) to the difference in the corresponding ET samples (ΔET). The two final WP, $WP_{B\text{-}ET}$ and $WP_{Y\text{-}ET}$, were calculated as ratios of final biomass (B) and yield (Y) to total ET (Ran et al., 2017). The two irrigation water productivity indicators, $WP_{B\text{-}I}$ and $WP_{Y\text{-}I}$, were the ratios of final biomass (B) and yield (Y) to total irrigation depth (I) (Cai et al., 2021).

N seed production efficiency (NUE_g) was obtained by dividing Y by total aboveground N uptake (U_B). N harvest index (NHI) was the ratio of grain N accumulation (U_Y) to U_B (Che et al., 2015). The N recovery (RE_N) was the difference between the N uptake of the N treatment (U_{BN}) and the N uptake of the non-N treatment (U_{B0}) divided by the N application rate (N_a) (Wang et al., 2019). Yield-based N use efficiency (NUE_{yield}) was calculated as the ratio of yield (Y) to the applied N rate (Na) (Ye et al., 2022). The actual measured ET-based N uptake rate ($N_{uptake\text{-}ET}$) was calculated as the ratio of the N uptake between two adjacent samples of aboveground biomass (ΔU_B) to the corresponding ET difference (ΔET).

2.4. Water productivity (WP) models

2.4.1. The $WP_{KR\text{-}L}$ model

The Logistic equation (Thornley, 1976) is applied to the relationship between crop biomass growth and evapotranspiration accumulation as follows:

$$B_t = f\left(ET\right) = \frac{B_0 B_m}{B_0 + (B_m - B_0)e^{-\delta ET}} \tag{1}$$

where B_t is the standardized biomass accumulation $\Sigma(\Delta B_i/B_{W1N150})$, ΔB_i is the biomass increment along the growth period of maize for the ith treatment, B_{W1N150} is the final biomass of the treatment without water and N stress, B_m is the standardized final biomass for each treatment (B/B_{W1N150}), B represents the final biomass for each treatment, B_0 is the standardized initial biomass, δ is the potential biomass growth index, ET is the standardized cumulative crop evapotranspiration $\Sigma(\Delta ET_i/ET_{W1N150})$, ΔET_i is the time series evapotranspiration increment along the growth period for the ith treatment, and ET_{W1N150} is the final ET of the treatment without water and N stress.

$WP_{KR\text{-}L}$ model is a nonlinear dynamic model based on the Logistic equation, which is obtained by deriving *f*(ET) as in (Ran et al., 2019):

$$WP_{KR-L} = \frac{B_m B_0 \delta (B_m - B_0)e^{-\delta ET}}{\left[B_0 + (B_m - B_0)e^{-\delta ET}\right]^2} \tag{2}$$

2.4.2. The $WP_{KR\text{-}S}$ model

The Sigmoid equation (Thornley, 1976) is applied to the relationship between crop biomass accumulation and evapotranspiration as follows:

$$B_t = g\left(ET\right) = B_m \frac{(ET/ET_c)^\eta}{1 + (ET/ET_c)^\eta} \tag{3}$$

where ET_c is the ET value corresponding to the half-maximum response of biomass, and η is a constant.

$WP_{KR\text{-}S}$ model is a nonlinear dynamic WP model derived from the Sigmoid equation by deriving g(ET) (Ran et al., 2019):

$$WP_{KR-S} = \frac{\eta B_m {ET_c}^{\eta} ET^{(\eta-1)}}{\left({ET_c}^{\eta} + ET^{\eta}\right)^2} \tag{4}$$

2.5. The N uptake model based on evapotranspiration

Santachiara et al. (2018) showed that biomass accumulation of maize at different growth stages is significantly related to N uptake and its utilization efficiency. Here, we choose the N dilution curve to quantify the relationship between N status and maize growth, based on the equation proposed by Lemaire and Salette (1984):

$$N_{uptake} = \alpha(B_t)^{1-\beta} \tag{5}$$

where N_{uptake} is aboveground N accumulation, parameter α is N uptake per unit of aboveground biomass, and parameter 1-β is the isokinetic coefficient (ratio of relative rates) between N uptake and its growth rate. α is related to the amount of N applied and 1-β is determined by the N nutrient status (Salette et al., 1982).

Different types of N uptake models based on ET are developed by taking the Logistic model (Eq. (1)), Sigmoid model (Eq. (3)), and Linear model into Eq. (5), respectively:

$$N_{uptake} = \alpha(B_{ti})^{1-\beta} \tag{6}$$

where B_{ti} represents the simulated biomass using the Logistic model, Sigmoid model, and Linear model, respectively.

The N uptake rate ($N_{uptake-ET}$) model based on ET can be obtained by deriving ET in Eq. (6) as follows:

$$N_{uptake-ET} = \frac{d(N_{uptake})}{d(ET)} = \alpha\left(1-\beta\right)(B_{ti})^{-\beta}\frac{d(B_{ti})}{d(ET)} = \alpha\left(1-\beta\right)(B_{ti})^{-\beta}WP_{ti} \tag{7}$$

where WP_{ti} represents the simulated WP using the Logistic model, Sigmoid model, and Linear model, respectively.

2.6. Statistical analysis

Five statistical indices are adopted to estimate the accuracy of the models. They are coefficient of determination (R^2), adjusted coefficient of determination (R^2_{adj}), root mean square error (RMSE), normalized root mean square error (NRMSE), and Willmott's index of agreement (d). Their formulas can be found in Ran et al. (2019). R^2 can show the proportion of variance in the dependent variable that is explained by the model. R^2_{adj} is adjusted R^2, which takes into account the number of parameters and the sample size. RMSE and NRMSE are adopted to represent overall errors between the simulated and measured values. d is used to measure the agreement between simulated and measured time series data in this study.

3. Results

3.1. Effects of water and N stress on maize growth and resource use efficiency

Water stress reduced the final biomass (B), grain yield (Y), and harvest index (HI) by 15.4%, 36.5%, and 26.9% on average, respectively (Fig. 1). N stress showed a less negative impact compared to water stress, reducing B, Y, and HI by 12.3%, 18.7%, and 8.6% on average, respectively (Fig. 1). Yield loss due to N reduction at high and low irrigation levels was 14.3% and 40.1%, respectively. On the other hand, yield loss caused by the decrease of irrigation depth at N150 and N0 rates was 47.3% and 64.8%, respectively (Fig. 2). The total evapotranspiration (ET) of different treatments ranged from 403 to 563 mm, which decreased by 17.4% and 3.3% due to water and N stresses on average, respectively (Fig. 3). WP_{B-ET} and WP_{Y-ET} were 3.8–4.7 kg m^{-3} and 0.6–1.4 kg m^{-3}, respectively, with 247–428 mm irrigation and

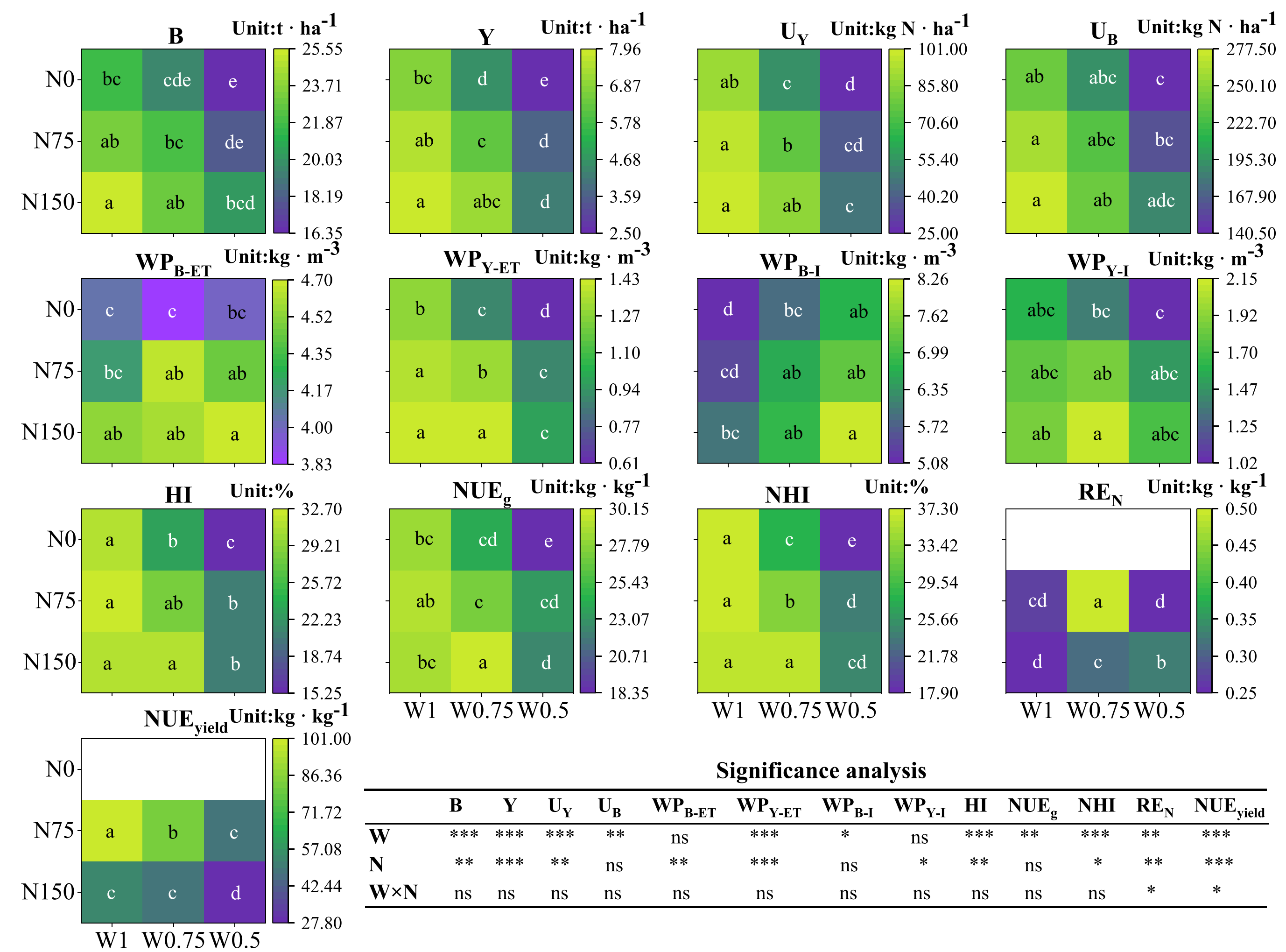

	B	Y	U_Y	U_B	WP_{B-ET}	WP_{Y-ET}	WP_{B-I}	WP_{Y-I}	HI	NUE_g	NHI	RE_N	NUE_{yield}
W	***	***	***	**	ns	***	*	ns	***	**	***	**	***
N	**	***	**	ns	**	***	ns	*	**	ns	*	**	***
W×N	ns	ns	ns	ns	ns	ns	ns	ns	ns	ns	ns	*	*

Fig. 1. Effects of water and nitrogen stress on aboveground biomass (B), yield (Y), seed N accumulation (U_Y), aboveground N accumulation (U_B), biomass-based water productivity (WP_{B-ET}), yield-based water productivity (WP_{Y-ET}), biomass-based irrigation water use efficiency (WP_{B-I}), yield-based irrigation water use efficiency (WP_{Y-I}), harvest index (HI), nitrogen seed production efficiency (NUE_g), nitrogen harvest index (NHI), nitrogen recovery efficiency (RE_N), and nitrogen fertilizer production efficiency (NUE_{yield}). W1, W0.75, and W0.5 represent full irrigation level, mild water stress level with 75% of W1 irrigation, and severe water stress level with 50% of W1 irrigation, respectively. N150, N75, and N0 represent N applications of 150, 75, and 0 kg N ha^{-1}, respectively. According to the LSD test, color blocks with the same letters are not significantly different ($P < 0.05$). * , * *, and * ** indicate significance at $P < 0.05$, $P < 0.01$, and $P < 0.001$ levels, respectively; ns, no significance.

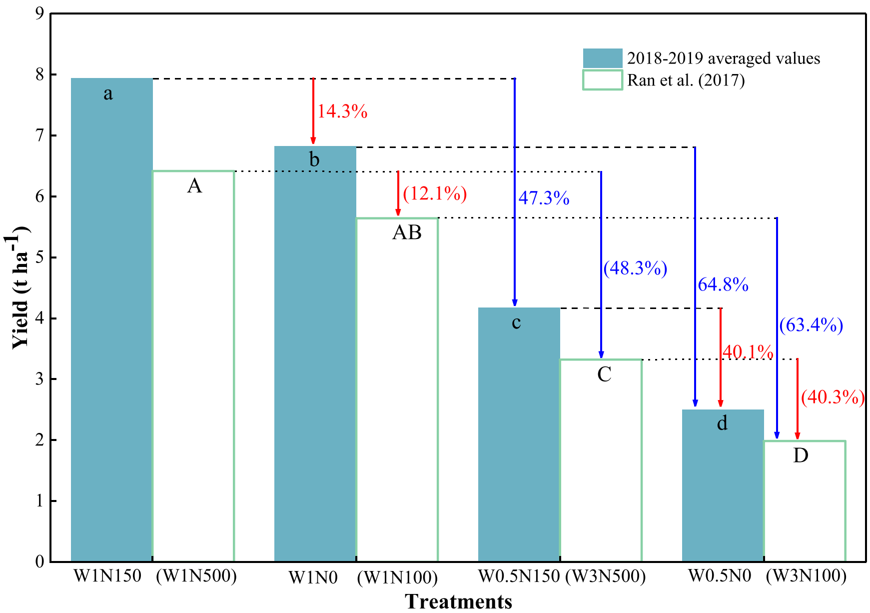

Fig. 2. Response of yield to water and N stress under the four extreme water and N treatments. The filled pillars represent the average yield in 2018 and 2019. The empty pillars represent the data from Ran et al. (2017). W1 and W0.5 represent full irrigation level and severe water stress level with 50% of W1 irrigation, respectively. N500, N150, N100, and N0 represent 500, 150, 100, and 0 kg N ha^{-1} N application, respectively. W1 and W3 in Ran et al. (2017) represent irrigated at 70–65% and 50–45% of field capacity, respectively. According to the LSD test, the treatments with the same letter are not significantly different ($p < 0.05$) in the same color bar graph.

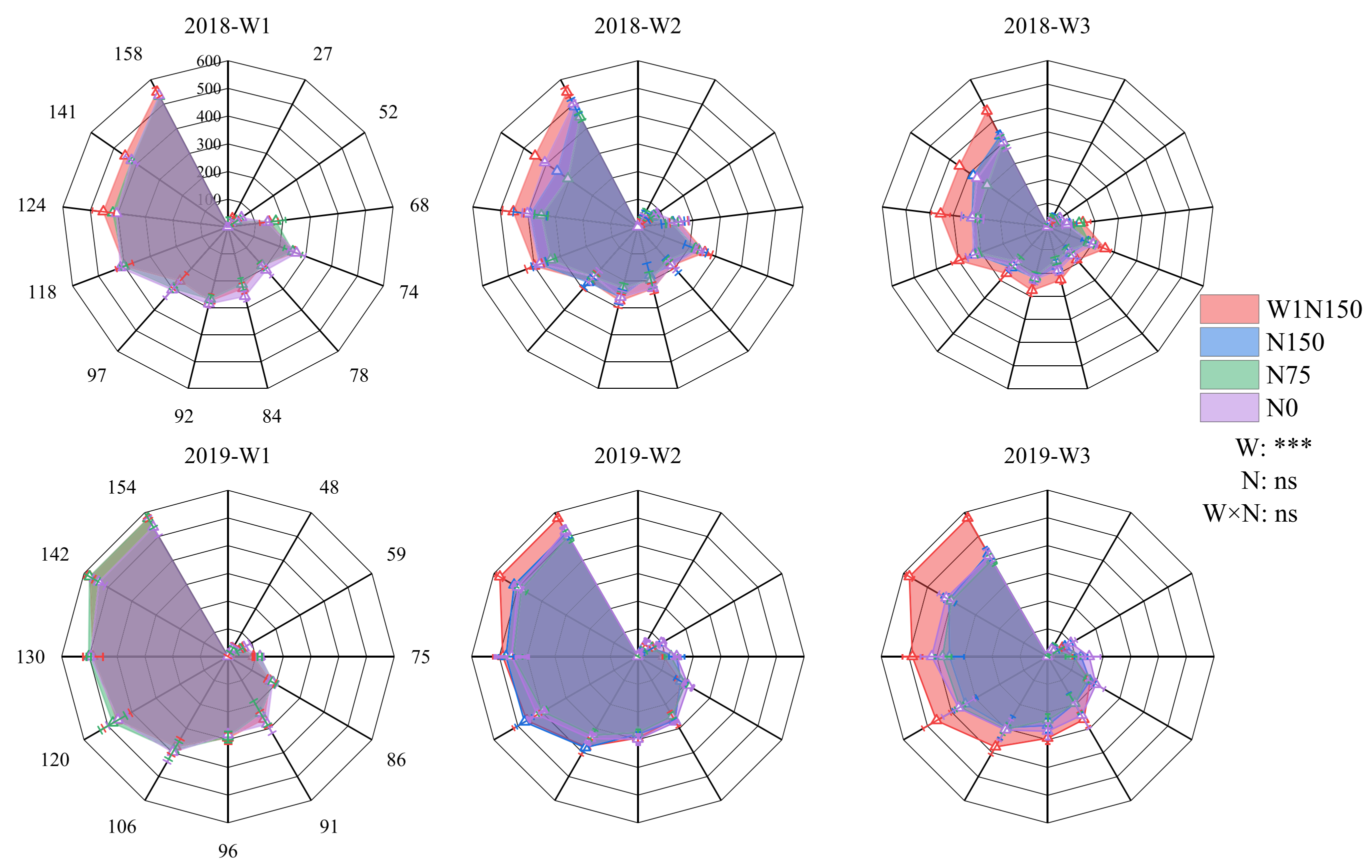

Fig. 3. Variation of maize evapotranspiration (ET) during the growth period under different irrigation and nitrogen treatments in 2018 and 2019. W1, W0.75, and W0.5 represent full irrigation level, mild water stress level with 75% of W1 irrigation, and severe water stress level with 50% of W1 irrigation, respectively. N150, N75, and N0 represent N applications of 150, 75, and 0 kg N ha^{-1}, respectively. The unit of ET is mm. Data 27–158 indicate days after sowing. * ** indicates significance at $P < 0.001$ level. ns, no significance.

0–150 kg N ha^{-1} fertilizer application. WP_{B-I} and WP_{Y-I} were 5.1–8.3 kg m^{-3} and 1.0–2.2 kg m^{-3}, respectively. Water productivity based on ET (WP_{ET}) and the corresponding water productivity based on irrigation depth (WP_I) were significantly correlated ($P < 0.05$) (Fig. 1). WP_{B-ET} slightly increased by 3.2% while WP_{Y-ET} significantly decreased by 24.2% under water stress conditions on average. N application increased WP_{B-ET} and WP_{Y-ET} by 9.1% and 16.5% on average, respectively (Fig. 4). The measured WP showed a single peak variation along the increase of ET, with the quadratic polynomial fitting (R^2 =0.23, d=0.62) being better than the linear regression (R^2 =0.00, d=0.05)

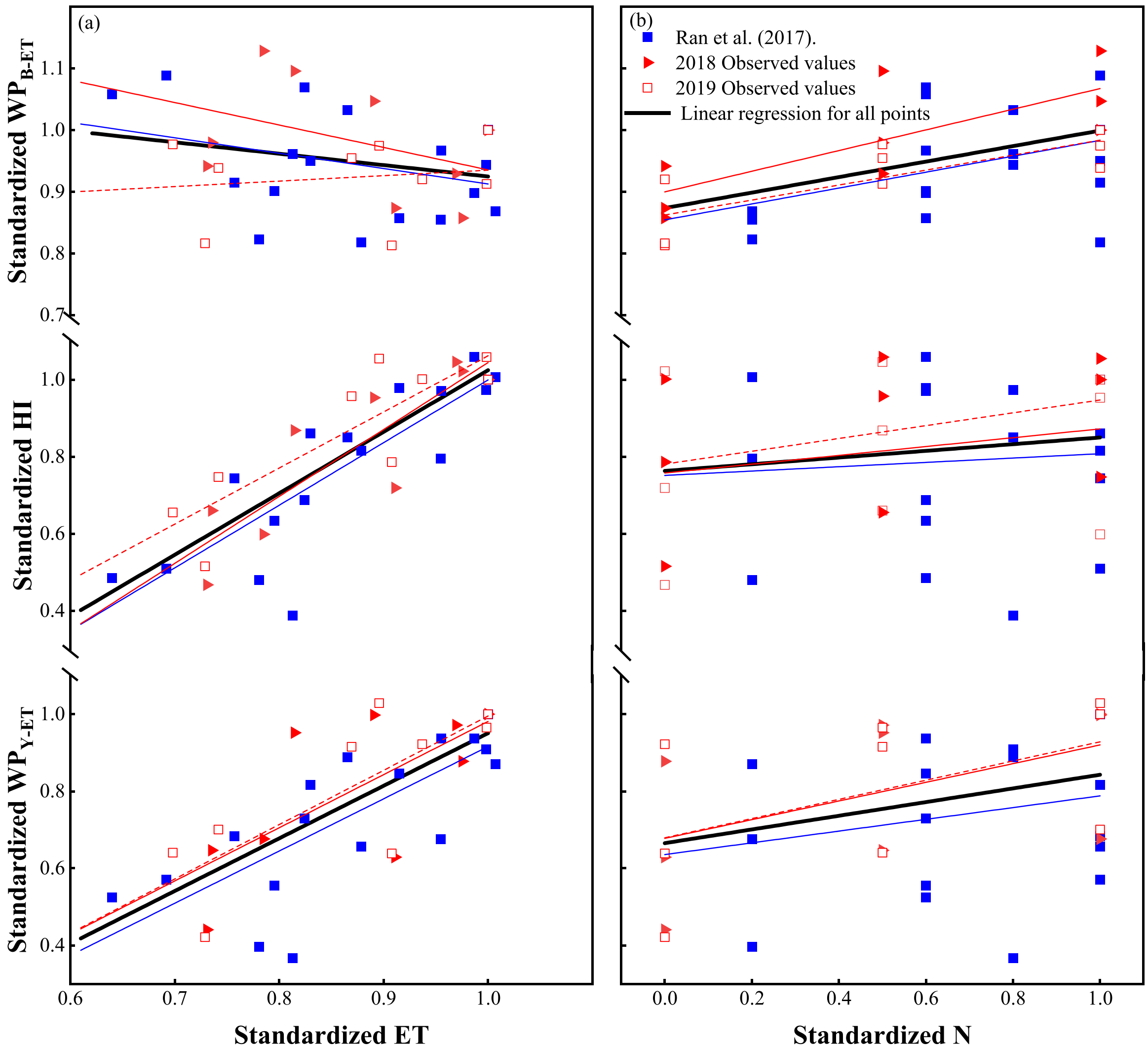

Fig. 4. Response of final biomass-based water productivity (WP_{B-ET}) and yield-based water productivity (WP_{Y-ET}) of maize to water and nitrogen stress. The solid blue line represents the linear fit of the data cited from Ran et al. (2017). The red dashed and solid lines represent linear fits of the data in 2018 and 2019, respectively. The bold black solid line represents the linear fit for all data.

(Fig. 5).

The aboveground N accumulation (U_B) and seed N accumulation (U_Y) of maize ranged from 140.5 to 277.5 kg N ha^{-1} and 25.0–101.0 kg N ha^{-1}, respectively (Fig. 1). The relationship between N accumulation and biomass was significantly correlated ($P < 0.01$) (Fig. 1). N application increased maize N content by 22.2% in the vegetative growth stage, and N uptake was reduced by 27.8% under irrigation and N stress conditions in the reproductive growth stage on average (Fig. 6). Overall, irrigation and N application improved N uptake of maize by 25.7% and 13.6% on average, respectively. The N seed production efficiency (NUE_g), N harvest index (NHI), yield-based N use efficiency (NUE_{yield}), and N recovery efficiency (RE_N) responding to the water and N combinations were 18.4–30.2 kg kg^{-1}, 17.9–37.3%, 27.8–101.0 kg kg^{-1}, and 0.3–0.5 kg kg^{-1}, respectively (Fig. 1). Increasing irrigation depth improved NUE_g, NUE_{yield}, and NHI, whereas full irrigation reduced RE_N (Fig. S2a and S2b). N application increased NUE_g and NHI by 8.3% and 10.5% on average, respectively, but decreased RE_N and NUE_{yield} by 12.2% and 44.8% on average, respectively (Fig. S2c and S2d).

3.2. Simulations of nonlinear dynamic WP models under water and N stress

The Logistic, Sigmoid, and Linear models well represented the relationship between biomass accumulation (B_t) and ET increasing along the growth period with $R^2 > 0.90$ (Table S2). For all the water and N treatments, the Logistic, Sigmoid, and Linear models showed similar high accuracy for quantifying the relationship between evapotranspiration accumulation and biomass growth process, with R^2 and NRMSE ranged from 0.96 to 0.99 and 7.3–16.4%, respectively (Fig. 7a and b, Table S2).

The simulated dynamic and static WP curves of maize during the growth period from the Logistic equation, Sigmoid equation, and Linear model are shown in Fig. 7c, d, and Fig. S3. The dynamic WP curve showed a single peak in the whole growth period, which was similar to the pattern of measured WP (Fig. 7). For W1N150, the d between the simulated WP of $WP_{KR\text{-}L}$ and $WP_{KR\text{-}S}$ models and measured WP were 0.64 and 0.73, which were higher than that of the Linear model (0.21). For W0.5N0, the d of the $WP_{KR\text{-}L}$ and $WP_{KR\text{-}S}$ models were 0.73 and 0.75, which were also higher than the 0.21 of the Linear model (Table S3). The $WP_{KR\text{-}S}$ model simulated 27.1% higher peak value of WP than the $WP_{KR\text{-}L}$ model, and also showed the peak 50.2% earlier (Fig. 7c). Water stress increased the peak values of $WP_{KR\text{-}L}$ and $WP_{KR\text{-}S}$ dynamic models by

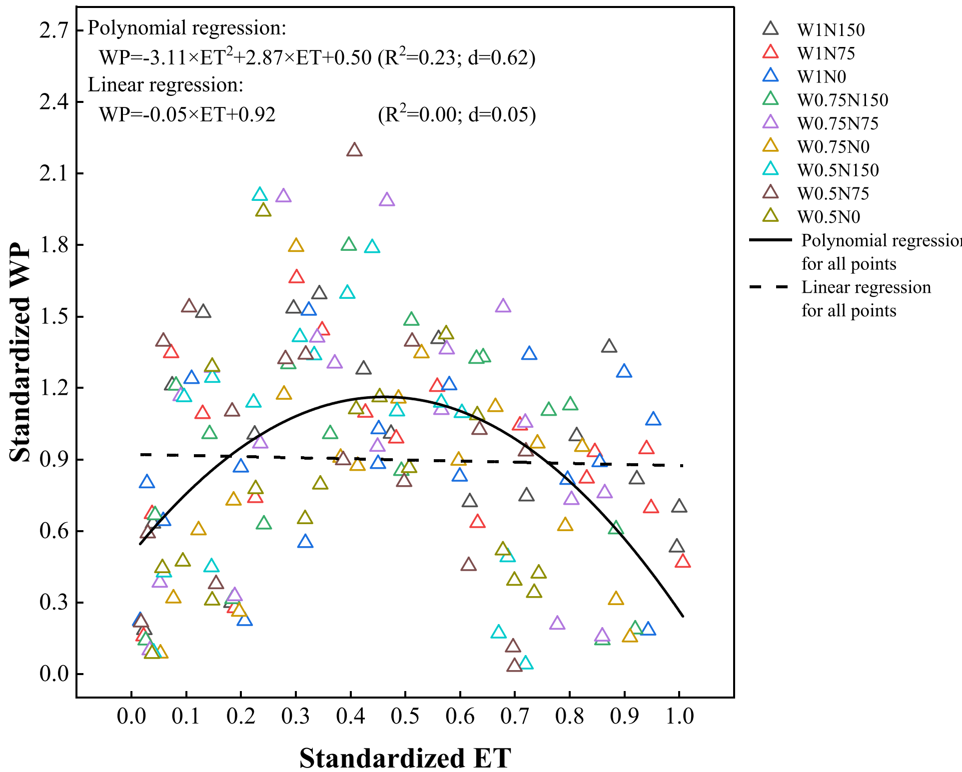

Fig. 5. Variation of measured water productivity (WP) against evapotranspiration (ET) in 2018 and 2019. W1, W0.75, and W0.5 represent full irrigation level, mild water stress level with 75% of W1 irrigation, and severe water stress level with 50% of W1 irrigation, respectively. N150, N75, and N0 represent N applications of 150, 75, and 0 kg N ha^{-1}, respectively. R^2 is the determination coefficient. d is the Willmott's index of agreement.

27.1% and 19.6% on average, respectively, and also resulted in earlier peaks (Fig. S3). N application increased dynamic WP at the whole growth stage (Fig. S3). The standardized Linear WP model simulation values varied from 0.9 to 1.1 under different irrigation and N treatments. Decreasing irrigation from 428 to 247 mm averagely increased 5.6% of the standardized WP values, and increasing N application from 0 to 150 kg N ha^{-1} averagely increased it by 19.1% (Table S2).

3.3. Performance of ET-based dynamic N uptake models

Logistic, Sigmoid, and Linear models showed similar high accuracy in describing the relationship between N uptake (N_{uptake}) and ET (Fig. 8a). Specifically, they were more accurate in quantifying the relationship between N_{uptake} and ET under non-stress and mild water and N stress treatments (R^2 >0.92, NRMSE<14.7%) than under the severe water and N stress treatments (0.77 <R^2 <0.84, 17.9%< NRMSE<23.9%) (Fig. 8a and Table S4). However, the derived ET-based N uptake rates from the Logistic, Sigmoid, and Linear models showed large residual errors in comparison to the measured values, with NRMSE exceeding 30% (Table S5). In the W1N150 treatment, the ET-based N uptake rates simulated by the Logistic model after derivation were 0.59, 1.25, and 0.19 at the initial, middle, and end growth stages, in comparison to the Sigmoid model after derivation of 0.96, 2.03, and 0.13. While for the W0.5N0 treatment, the Logistic and Sigmoid models for N uptake rates simulated by the Logistic and Sigmoid models after derivation were 0.37, 0.92, and 0.03, and 0.35, 1.35, and 0.3, respectively (Fig. 8b). The peak of the Sigmoid model after derivation appeared at standardized ET= 0.17, while it occurred at standardized ET= 0.42 for the Logistic model after derivation for the W1N150 treatment. Water stress increased the peak value and advanced the appearance time of the N uptake rate, while N stress did the opposite (Fig. S4a and S4b). The ET-based N uptake rate simulated by the Linear model after derivation showed a monotonic decrease for the whole growth stage, with the simulated values decreasing from 2.53 to 0.64, and from 2.10 to 0.43 along the growth period for the W1N150 and W0.5N0 treatments, respectively (Fig. 8b and Fig. S4c).

4. Discussion

4.1. The priority of water over nitrogen for maize production in arid northwest China

Compared to W1N150, water stress reduced yield (Y), final aboveground biomass (B), and harvest index (HI) by 36.5%, 15.4%, and 26.9% on average, respectively, while N stress reduced them by 18.7%, 12.3%, and 8.6%, respectively (Fig. 1). This indicates that water stress has a greater impact on Y, B, and HI comparing to N stress, and Y is more susceptible to water and N stress, which is similar to the results of Li et al. (2020). In addition, both our results and Ran et al. (2017) showed that N reduction had a greater impact on yield under water stress, and the decrease of irrigation depth caused more yield loss under zero N application than the N150 rate (Fig. 2). This indicates that further reduction of water and N resources will increase yield loss under water and N stress conditions in arid Northwest China. This result is different from Di Paolo, Rinaldi (2008) and Ogola et al. (2002), in which the negative effect of water deficit is greater with higher N application. The reason for the difference might be that adding more water and N resources can mitigate the negative effects of water and N stress on yield in an arid climate environment. Furthermore, we also found that water stress reduced seed N uptake (U_Y), aboveground N uptake (U_B), and N harvest index (NHI) by 42.9%, 25.7%, and 25.4% on average, respectively, while N stress reduced them less by 19.2%, 13.6%, and 9.2%, respectively (Fig. 1). This shows that water stress also has a greater impact on N use efficiency than N stress, which was similar to Li et al., 2022a,b. It is more important to prioritize the soil water content to promote crop N uptake and yield formation because soil water

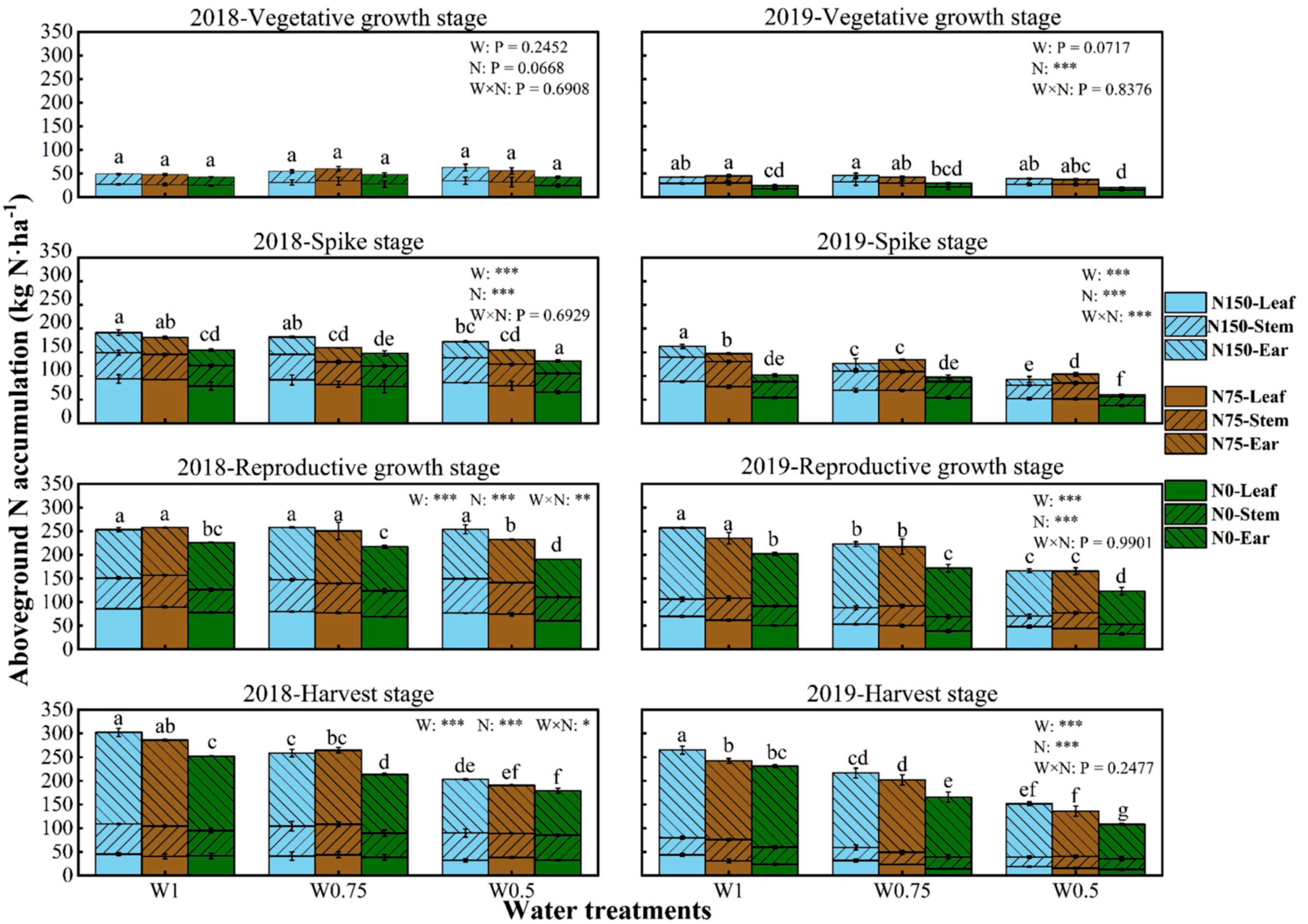

Fig. 6. Effect of water and nitrogen stress on nitrogen accumulation in different organs of maize at different growth stages in 2018 and 2019. W1, W0.75, and W0.5 represent full irrigation level, mild water stress level with 75% of W1 irrigation, and severe water stress level with 50% of W1 irrigation, respectively. N150, N75, and N0 represent N applications of 150, 75, and 0 kg N ha^{-1}, respectively. According to the LSD test, the treatments with the same letters are not significantly different ($p < 0.05$) in the same color bar graph. * , * *, and * ** indicate significance at $P < 0.05$, $P < 0.01$, and $P < 0.001$ levels, respectively.

effectiveness affects the availability of N and crop N uptake (Pandey et al., 2000). Thus, we conclude that water has priority over nitrogen for crop production in arid Northwest China, which is consistent with the findings of Ran et al. (2017).

4.2. *Response of WP and NUE to water and N stress*

Our results showed $WP_{Y\text{-}ET}$ of hybrid seed maize varied from 0.6 to 1.4 kg m^{-3}, which was slightly higher than the result of 0.4–1.2 kg m^{-3} in Ran et al. (2017). Water and N stress reduced $WP_{Y\text{-}ET}$ by 22.4% and 16.5% on average under border irrigation and mulching conditions in arid Northwest China, respectively (Fig. 1). Guo et al. (2022) revealed that $WP_{Y\text{-}ET}$ was reduced by 1.7% with water stress on drip irrigated hybrid maize in a semi-humid but drought-prone region (precipitation = 632 mm). Zhang et al. (2022) showed a reduction of $WP_{Y\text{-}ET}$ of 10.7% in N stress in mulched field maize in the semi-arid Loess Plateau (precipitation = 548 mm). These results show a smaller variation of $WP_{Y\text{-}ET}$ than our results in the arid environment (164 mm), which indicates that $WP_{Y\text{-}ET}$ might be more sensitive to water and N stress under an arid climate. On the other hand, our results showed $WP_{B\text{-}ET}$ varied from 3.8 to 4.7 kg m^{-3} (Fig. 1), higher than the 2.8–3.9 kg m^{-3} in Ran et al. (2017), which is also true for $WP_{Y\text{-}ET}$. The systematic higher $WP_{B\text{-}ET}$ and $WP_{Y\text{-}ET}$ might be due to the different varieties in the two studies. In addition, N stress reduced $WP_{B\text{-}ET}$ by 9.1% on average, while water stress increased it by 3.2% instead (Fig. 4). The variation of $WP_{B\text{-}ET}$ is smaller than that in Roja et al. (2021) (11.0%) and Adeboye et al. (2021) (29.6%).

When comparing the responses of $WP_{B\text{-}ET}$ and $WP_{Y\text{-}ET}$ to water stress, we found that $WP_{Y\text{-}ET}$ decreased significantly with increasing water stress (Fig. 4), which is consistent with the results of other studies (Ran et al., 2017; Wang et al., 2019; Xing et al., 2021). However, $WP_{B\text{-}ET}$ tended to slightly (but non-significantly) increase along with increased water stress (Fig. 4), which is similar to the results of Ran et al. (2017). This indicates that $WP_{B\text{-}ET}$ and $WP_{Y\text{-}ET}$ respond differently to water stress. The different response between $WP_{Y\text{-}ET}$ and $WP_{B\text{-}ET}$ to ET is related to HI, which is the ratio of $WP_{Y\text{-}ET}$ to $WP_{B\text{-}ET}$. Our results showed that HI decreased with the increase of water and N stress, and the negative effect of water stress was more pronounced because of a greater slope (Fig. 4). Since $WP_{B\text{-}ET}$ is more stable than $WP_{Y\text{-}ET}$ in response to water stress (Ran et al., 2017), the change of $WP_{Y\text{-}ET}$ should be consistent with HI (Payero et al., 2006; Howell and Douglas, 1990). Thus, $WP_{Y\text{-}ET}$ is reduced because of the potential HI being decreased by water stress. Su et al. (2020) reported that water stress reduces $WP_{Y\text{-}ET}$ through yield loss. Several studies have shown that water stress has a facilitative effect on standardized water productivity (ratio of biomass to evapotranspiration or evapotranspiration) (Katerji et al., 2013; Hellal et al., 2019; Adeboye et al., 2021), which was similar to the response of $WP_{B\text{-}ET}$ to water stress in our study. On the other hand, applying N had a stimulatory effect on both $WP_{Y\text{-}ET}$ and $WP_{B\text{-}ET}$ (Fig. 4). The increase of $WP_{Y\text{-}ET}$ and $WP_{B\text{-}ET}$ by N application might be related to the promotion of physiological and biochemical processes including root distribution and seed filling (Pico et al., 2021; Ye et al., 2022; Zhang et al., 2022).

Irrigation significantly ($P < 0.01$) affected N uptake and utilization

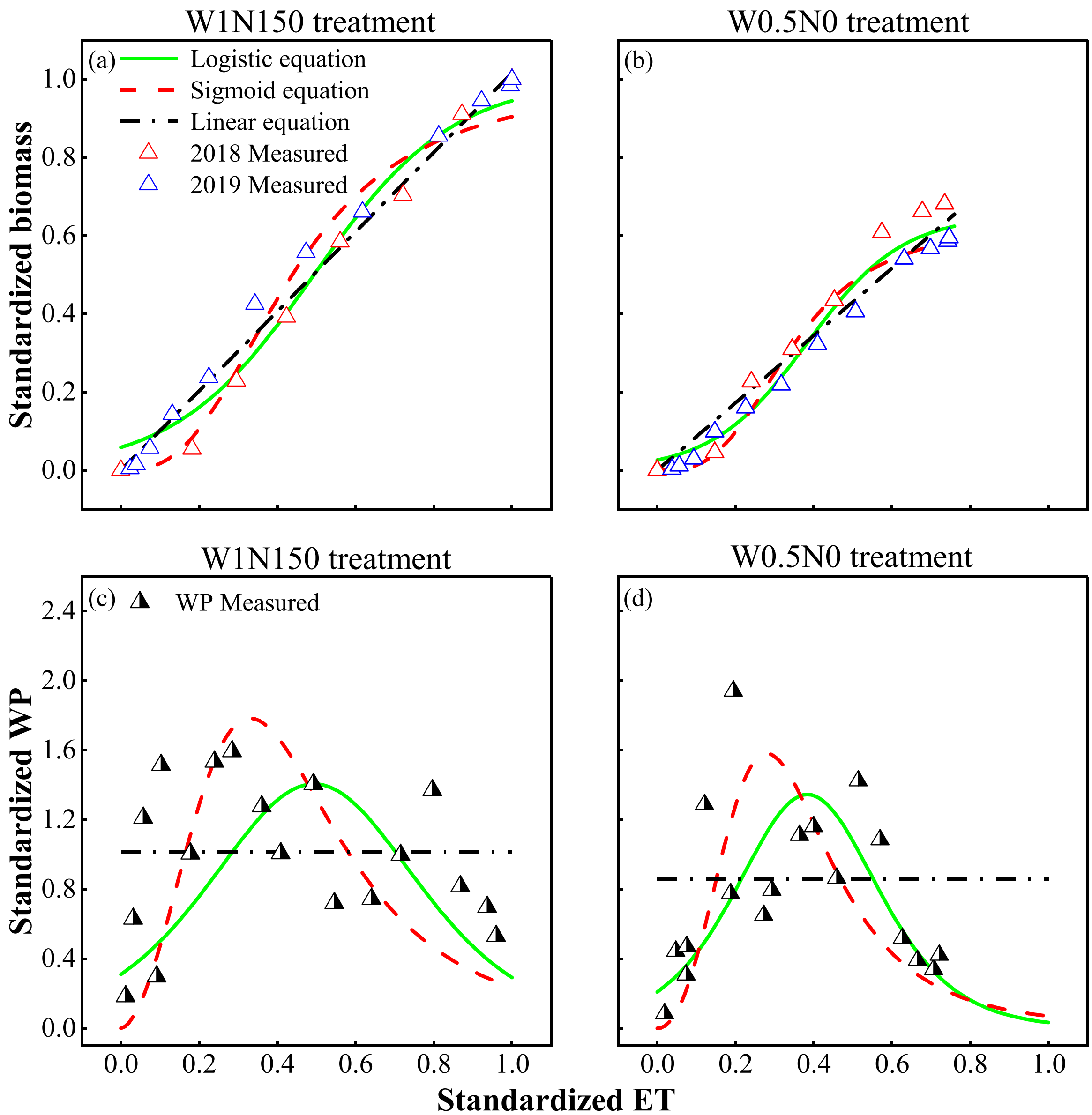

Fig. 7. Simulations of Logistic, Sigmoid, and Linear models and the corresponding derived water productivity (WP) for the high irrigation and high N treatment (W1N150) and low irrigation and non-N treatment (W0.5N0).

efficiency, and water stress reduced NUE_g, NUE_{yield}, RE_N, and NHI (Fig. 1), which is consistent with other studies (Jégo et al., 2022; Lai et al., 2022; Li et al., 2022b). Water stress also decreased aboveground N uptake (U_B) and seed N accumulation (U_Y), limited N assimilation, and reduced N utilization of maize. On the other hand, N application improved NUE_g and NHI while decreasing NUE_{yield} and RE_N (Fig. 1 and Fig. S2). This is because N application increases the availability of N to maize, resulting in an increased N uptake (Ashraf et al., 2016). However, high N application is more likely to lead to N fertilizer mineralization, resulting in decreased N fertilizer recovery efficiency (Wang et al., 2019).

4.3. Strength of nonlinear dynamic water productivity models

Many studies have simplified the relationship between biomass accumulation (B_t) and transpiration (T) or evapotranspiration (ET) as a linear relationship, which means its slope, WP, is taken as a fixed value during the growth period (Steduto et al., 2007; Tsegay et al., 2011; Adeboye et al., 2017). However, our measured WP values were not constant along the growth period, which showed a single peak trend and had a higher correlation and agreement to the quadratic curve in comparison to the linear regression (Fig. 5), similar to the dynamic process that Hsiao et al. (2009) found, i.e., increase-stable-decrease. This dynamic process was further quantified by Ran et al. (2019) using Logistic and Sigmoid models, where nonlinear dynamic WP models were found to improve the simulation accuracy of biomass under non-stress conditions. From the average results for all treatments, our results showed that the Logistic, Sigmoid, and Linear models had similar high accuracy for quantifying the relationship between biomass growth and ET accumulation (Fig. 7a, b, and Table S2). However, the derived WP values from the nonlinear dynamic models were more in line with the single peak variation of the measured WP during the growth period, with the agreement index (d) improving from 0.21 to 0.65–0.75 in comparison to the Linear model (Fig. 5). Thus, from the perspective of WP variation, the nonlinear Logistic and Sigmoid models were more compatible with the relationship between biomass and evapotranspiration than the Linear model (Fig. 7c, d, and Table S3). However, some WP points in Fig. 5 were divergent, which means these measured WP values

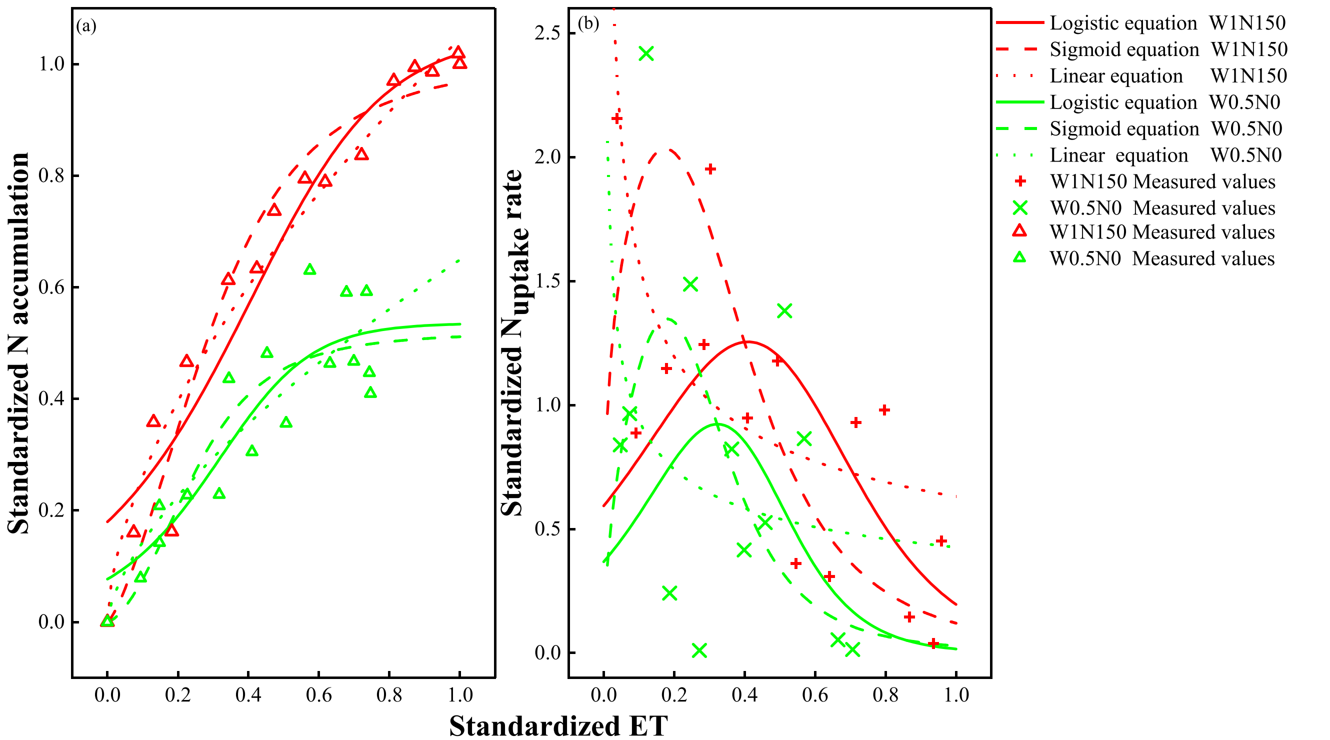

Fig. 8. Performance of ET-based N uptake models and the corresponding derived ET-based N uptake rate for the high irrigation and high N treatment (W1N150) and low irrigation and non-N treatment (W0.5N0).

calculated using the intervals between every two adjacent samples might have large potential uncertainty. The errors might come from the increments of both evapotranspiration and biomass calculated using the intervals between every two adjacent samples.

The magnitude and the appearance of the peak of simulated dynamic WP were affected by water and N stresses (Fig. 7c, d, and Fig. S3). Water stress increased the peak value and growth rate of WP at the vegetative growth stage, and the severer the stress, the more significant the increase. On the contrary, the WP decreased rapidly due to water stress at the reproductive growth stage, and the rate of decrease was significantly related to the degree of water stress (Fig. S3). N application increased the dynamic WP at the whole growth stage under water stress conditions, but the current N application has limited benefits for alleviating the effect of water stress on WP. The simulation results of nonlinear WP models showed that the WP_{KR-L} and WP_{KR-S} models underestimated WP in the vegetative growth stage, and the WP_{KR-S} simulated results were higher than the WP_{KR-L} with a larger peak value, while the WP_{KR-S} simulated results were lower than the WP_{KR-L} during the reproductive growth phase (Fig. 7c and d). The difference might be related to the different properties of the first-order derivative of Logistic and Sigmoid functions.

4.4. Feasibility of ET-based N uptake rate models

Many studies have found that N uptake and utilization of maize are affected by water availability (Jégo et al., 2022; Ye et al., 2022). The N cycling is regulated by water, which affects the effectiveness and availability of soil N for plant uptake (Ashraf et al., 2016; Li et al., 2019; Qiang et al., 2022; Zhang et al., 2022). Our results showed that the Logistic, Sigmoid, and Linear models had acceptable accuracy for quantifying water consumption and N uptake under different irrigation and N treatments (Table S4). R^2 and NRMSE of the three models were higher than 0.92 and lower than 14.7% for no or mild water and N stress, and were also higher than 0.79 and lower than 23.9% for heavy water and N stress. (Fig. 8a and Table S4). Our results also indicate that the three ET-based N uptake models have high feasibility and accuracy for quantifying water status and N uptake of maize throughout the growth period. Thus, we suggest that N accumulation can be quantified through evapotranspiration as an alternative approach.

The relationship between ET and N uptake in different growth stages of maize was significantly correlated ($P < 0.01$, Fig. 8a). The Logistic and Sigmoid models also showed single-peaked variation in ET-based N uptake rates, and the latter simulated values were larger than the former in the whole growth period. The form of the single-peaked curve variation is similar to the results of dynamic WP during the growing period. In contrast, the ET-based N uptake rate of the standardized Linear model showed a monotonically decreasing form of variation (Fig. 8b and Fig. S5). This indicates that the pattern of simulated N uptake rates from ET-based N uptake models depends on the quantitative relationship between biomass and ET. Unfortunately, the pattern of ET-based N uptake rates was not clearly matched in this study, which might be caused by the uncertainty of measured N uptake rates (Fig. 8b). Further study is needed to improve the ET-based N uptake rate model.

4.5. Implications and perspectives

Water and N are two key factors for agricultural production (Ran et al., 2017). WP is a key link between crop production and water consumption, especially for arid regions where agriculture heavily depends on irrigation. Here, we demonstrated that final WP_{B-ET} and WP_{Y-ET} respond differently to water stress, and improved the non-linear dynamic WP models under water and N stress. This deepens our understanding of the relationship between crop water consumption and dry matter accumulation. Furthermore, we have developed three ET-based N uptake models, and intend to predict the nitrogen uptake of maize through water consumption under different levels of N application during the growth period. This provides a new perspective for evaluating plant N status. Thus, these results closely link resource inputs and agricultural outputs, which is useful for optimizing irrigation and N application management and improving resources use efficiency. They are also beneficial for the adaptation of agricultural practices, and sustainable maintenance or increase of agricultural productivity in climate-smart agriculture (FAO, 2012).

The nonlinear dynamic WP models and the ET-based N uptake models were evaluated using field experiments of maize in arid Northwest China in 2018 and 2019. Further evaluation is needed on other crops, climates, and regions with longer time series data. In addition, the irrigation depth and N application are limited to 247–428 mm and 0–150 kg N ha^{-1}, respectively. It is also necessary to add more water and N treatments and sampling frequency to further evaluate model parameters in the future. The measured values of WP and N_{uptake} rates calculated using the intervals between every two adjacent samples might have large potential uncertainty, which could cause model evaluation difficulties and needs further study.

The nonlinear dynamic WP models were found to be more consistent in representing the biological process of WP than the Linear model; however, the nonlinear models are more complicated and involve more parameters, making model calibration and interpretation more complex. The Linear model simplifies the growth process and ignores the dynamic change of WP, but the calculation is relatively simple and has acceptable simulation accuracy. Therefore, model selection depends on the specific needs of different practical applications. The nonlinear dynamic WP models and the ET-based N uptake models have the potential to be coupled with crop models and machine learning to improve the accuracy of crop growth simulation under stress conditions. Investigating the sensitivity and uncertainty of the parameters in the developed models, following the framework developed by Ran et al. (2022), is also of interest.

5. Conclusion

Water stress had a larger impact than N stress on the growth, yield and N uptake of maize in arid Northwest China. Biomass-based water productivity ($WP_{B\text{-}ET}$) and yield-based water productivity ($WP_{Y\text{-}ET}$) responded differently to water stress but similarly to N stress because HI was more sensitive to water stress than N stress. The Logistic, Sigmoid, and Linear models had similar high accuracy in quantifying the relationship between water consumption and crop growth, but the derived nonlinear dynamic WP models were more in line with the single peak variation of measured WP during the growth period. The developed ET-based N accumulation model was able to quantify N uptake through water consumption.

Declaration of Competing Interest

The authors declare that they have no known competing financial interests or personal relationships that could have appeared to influence the work reported in this paper.

Data Availability

Data will be made available on request.

Acknowledgements

We thank the anonymous reviewers and editor for their time to review this manuscript. This work is financially supported by the National Natural Science Foundation of China (51809216), and the National Field Scientific Observation and Research Station on Efficient Water Use of Oasis Agriculture in Wuwei of Gansu Province (No. KF2021005).

Appendix A. Supporting information

Supplementary data associated with this article can be found in the online version at doi:10.1016/j.agwat.2023.108370.

References

Adeboye, O.B., Schultz, B., Adekalu, K.O., Prasad, K., 2017. Modelling of response of the growth and yield of soybean to full and deficit irrigation by using Aquacrop. Irrig. Drain. 66 (2), 192–205.

Adeboye, O.B., Schultz, B., Adeboye, A.P., Adekalu, K.O., Osunbitan, J.A., 2021. Application of the AquaCrop model in decision support for optimization of nitrogen fertilizer and water productivity of soybeans. Inf. Process. Agric. 8 (3), 419–436.

Ashraf, U., Salim, M.N., Alam, S.H.E.R., Aqil, K.H.A.N., Shenggang, P.A.N., Xiangru, T.A. N.G., 2016. Maize growth, yield formation and water-nitrogen usage in response to varied irrigation and nitrogen supply under semi-arid climate. Turk. J. Field Crops 21 (1), 87.

Cai, Y., Wu, P., Zhu, D., Zhang, L., Zhao, X., Gao, X., Ge, M., Song, X., Wu, Y., Dai, Z., 2021. Subsurface irrigation with ceramic emitters: An effective method to improve apple yield and irrigation water use efficiency in the semiarid Loess Plateau. Agric., Ecosyst. Environ. 313, 107404.

Che, S., Zhao, B., Li, Y., Yuan, L., Li, W., Lin, Z., Hu, S., Shen, B., 2015. Review grain yield and nitrogen use efficiency in rice production regions in China. J. Integr. Agric. 14 (12), 2456–2466.

Di Paolo, E., Rinaldi, M., 2008. Yield response of corn to irrigation and nitrogen fertilization in a Mediterranean environment. Field Crops Res. 105 (3), 202–210.

El-Sanatawy, A.M., Ash-Shormillesy, S.M., Qabil, N., Awad, M.F., Mansour, E., 2021. Seed halo-priming improves seedling vigor, grain yield, and water use efficiency of maize under varying irrigation regimes. Water 13 (15), 2115.

FAO, 2012. Towards climate change adaptation: Strengthening capacities of farmers to adapt to climate change through land and water management in Sub-saharan Africa. Food and Agriculture Organization of the United Nations,.

Guo, J., Fan, J., Xiang, Y., Zhang, F., Yan, S., Zhang, X., Zheng, J., Li, Y., Tang, Z., Li, Z., 2022. Coupling effects of irrigation amount and nitrogen fertilizer type on grain yield, water productivity and nitrogen use efficiency of drip-irrigated maize. Agric. Water Manag. 261, 107389.

Hellal, F., Mansour, H., Abdel-Hady, M., El-Sayed, S., Abdelly, C., 2019. Assessment water productivity of barley varieties under water stress by AquaCrop model. AIMS Agric. Food 4 (3), 501–517.

Howell, G., Douglas, J.Y., 1990. The evolution of interactive fiction. Comp. Ass. Lang. Learn. 2 (1), 93–109.

Hsiao, T.C., Heng, L., Steduto, P., Rojas-Lara, B., Raes, D., Fereres, E., 2009. AquaCrop-the fao crop model to simulate yield response to water: iii: Parameterization and testing for maize. Agron. J. 101 (3), 448–459.

Jégo, G., Sansoulet, J., Pattey, E., Beaudoin, N., Bélanger, G., Ziadi, N., Tremblay, C., Grant, G., Tremblay, O'Donovan, J., Harker, K.N., Blackshaw, R., Johnson, E., Justes, E., 2022. Determination of nitrogen dilution curves of corn, canola, and spring wheat in Canada using classical and Bayesian approaches. Eur. J. Agron. 135, 126481.

Kang, J., Hao, X., Zhou, H., Ding, R., 2021. An integrated strategy for improving water use efficiency by understanding physiological mechanisms of crops responding to water deficit: Present and prospect. Agric. Water Manag. 255, 107008.

Kang, S., Shi, W., Zhang, J., 2000. An improved water-use efficiency for maize grown under regulated deficit irrigation. Field Crops Res. 67 (3), 207–214.

Kang, S., Hao, X., Du, T., Tong, L., Su, X., Lu, H., Li, X., Huo, Z., Li, S., Ding, R., 2017. Improving agricultural water productivity to ensure food security in China under changing environment: From research to practice. Agric. Water Manag. 179, 5–17.

Katerji, N., Campi, P., Mastrorilli, M., 2013. Productivity, evapotranspiration, and water use efficiency of corn and tomato crops simulated by AquaCrop under contrasting water stress conditions in the Mediterranean region. Agric. Water Manag. 130, 14–26.

Lai, Z., Fan, J., Yang, R., Xu, X., Liu, L., Li, S., Zha, F., Li, Z., 2022. Interactive effects of plant density and nitrogen rate on grain yield, economic benefit, water productivity and nitrogen use efficiency of drip-fertigated maize in northwest China. Agric. Water Manag. 263, 107453.

Lemaire, G., Salette, J., 1984. Relationship between growth and nitrogen uptake in a pure grass stand. I. Environmental effects. Agronomie 4, 423–430.

Li, C., Feng, H., Luo, X., Li, Y., Wang, N., Wu, W., Zhang, T., Dong, Q., Siddique, K.H.M., 2022a. Limited irrigation and fertilization in sand-layered soil increases nitrogen use efficiency and economic benefits under film mulched ridge-furrow irrigation in arid areas. Agric. Water Manag. 262, 107406.

Li, R., Hu, D., Ren, H., Yang, Q., Dong, S., Zhang, J., Zhao, B., Liu, P., 2022b. How delaying post-silking senescence in lower leaves of maize plants increases carbon and nitrogen accumulation and grain yield. Crop J. 10 (3), 853–863.

Li, Y., Li, Z., Cui, S., Chang, S.X., Jia, C., Zhang, Q., 2019. A global synthesis of the effect of water and nitrogen input on maize (Zea mays) yield, water productivity and nitrogen use efficiency. Agric. For. Meteorol. 268, 136–145.

Li, Y., Cui, S., Zhang, Z., Zhuang, K., Wang, Z., Zhang, Q., 2020. Determining effects of water and nitrogen input on maize (Zea mays) yield, water-and nitrogen-use efficiency: A global synthesis. Sci. Rep. 10 (1), 1–12.

Liao, Q., Ding, R., Du, T., Kang, S., Tong, L., Li, S., 2022. Stomatal conductance drives variations of yield and water use of maize under water and nitrogen stress. Agric. Water Manag. 268, 107651.

Liu, Z., Hao, Z., Sha, Y., Huang, Y., Guo, W., Ke, L., Chen, F., Yuan, L., Mi, G., 2022. High responsiveness of maize grain yield to nitrogen supply is explained by high ear growth rate and efficient ear nitrogen allocation. Field Crops Res. 286, 108610.

Lu, J., Ma, L., Hu, T., Geng, C., Yan, S., 2022. Deficit drip irrigation based on crop evapotranspiration and precipitation forecast improves water-use efficiency and grain yield of summer maize. J. Sci. Food Agric. 102 (2), 653–663.

Miao, X., Miao, Y., Liu, Y., Tao, S., Zheng, H., Wang, J., Wang, W., Tang, Q., 2022. Measurement of nitrogen content in rice plant using near infrared spectroscopy

combined with different PLS algorithms. Spectrochim. Acta Part A: Mol. Biomol. Spectrosc. 284, 121733.
National Data, 2022. https://data.stats.gov.cn/.
Ogola, J.B.O., Wheeler, T.R., Harris, P.M., 2002. Effects of nitrogen and irrigation on water use of maize crops. Field Crops Res. 78 (2–3), 105–117.
Pandey, R.K., Maranville, J.W., Admou, A., 2000. Deficit irrigation and nitrogen effects on maize in a Sahelian environment: I. Grain yield and yield components. Agric. Water Manag. 46 (1), 1–13.
Payero, J.O., Melvin, S.R., Irmak, S., Tarkalson, D., 2006. Yield response of corn to deficit irrigation in a semiarid climate. Agric. Water Manag. 84 (1–2), 101–112.
Pico, L.B.O., Zhang, C., Vyn, T.J., 2021. The central role of ear nitrogen uptake in maize endosperm cell and kernel weight determination during the lag period. Field Crops Res. 273, 108285.
Qiang, S., Zhang, Y., Zhao, H., Fan, J., Zhang, F., Sun, M., Gao, Z., 2022. Combined effects of urea type and placement depth on grain yield, water productivity and nitrogen use efficiency of rain-fed spring maize in northern China. Agric. Water Manag. 262, 107442.
Ran, H., Kang, S., Li, F., Du, T., Ding, R., Li, S., Tong, L., 2017. Responses of water productivity to irrigation and N supply for hybrid maize seed production in an arid region of Northwest China. J. Arid Land 9 (4), 504–514.
Ran, H., Kang, S., Li, F., Du, T., Tong, L., Li, S., Ding, R., Zhang, X., 2018. Parameterization of the AquaCrop model for full and deficit irrigated maize for seed production in arid Northwest China. Agric. Water Manag. 203, 438–450.
Ran, H., Kang, S., Hu, X., Li, F., Du, T., Tong, L., Li, S., Ding, R., Zhou, Z., Parsons, D., 2019. Newly developed water productivity and harvest index models for maize in an arid region. Field Crops Res. 234, 73–86.
Ran, H., Kang, S., Hu, X., Yao, N., Li, S., Wang, W., Galdos, M.V., Challinor, A.J., 2022. A framework to quantify uncertainty of crop model parameters and its application in arid Northwest China. Agric. For. Meteorol. 316, 108844.
Roja, M., Kumar, K., Ramulu, V., Deepthi, C., 2021. Modeling and evaluation of AquaCrop for maize (Zea mays L.) under full and deficit irrigation in semi-arid tropics. Indian J. Agric. Res. 55 (4), 428–433.
Salette, J., Lemaire, G., Robichet, J., 1982. Nitrogen and mineral uptake during regrowth of pure grass swards. Proc. 9th Gen. Meet. Eur. Grassl. Fed., Read. 5–9.
Santachiara, G., Salvagiotti, F., Gerde, J.A., Rotundo, J.L., 2018. Does biological nitrogen fixation modify soybean nitrogen dilution curves? Field Crops Res. 223, 171–178.
Steduto, P., Hsiao, T.C., Fereres, E., 2007. On the conservative behavior of biomass water productivity. Irrig. Sci. 25, 189–207.
Su, W., Ahmad, S., Ahmad, I., Han, Q., 2020. Nitrogen fertilization affects maize grain yield through regulating nitrogen uptake, radiation and water use efficiency, photosynthesis and root distribution. PeerJ 8, e10291.
Tarkalson, D.D., King, B.A.Bjorneberg, D.L., 2022. Maize grain yield and crop water productivity functions in the arid Northwest U.S. Agricultural Water Management, 264: 107513.
Thornley, J.H.M., 1976. Mathematical Models in Plant Physiology. Academic Press,, London, pp. 86–110.
Tsegay, A., Raes, D., Geerts, S.A.M., Vanuytrecht, E., Abraha, B., Deckers, J., Bauer, H., Gebrehiwot, K., 2011. Unravelling crop water productivity of tef (Eragrostis tef (Zucc.) Trotter) through AquaCrop in northern Ethiopia. Exp. Agric. 48 (2), 222–237.
Wang, T., Wang, Z., Zhang, J., Ma, K., 2022. An optimum combination of irrigation amount, irrigation water salinity and nitrogen application rate can improve cotton (for fiber) nitrogen uptake and final yield. Ind. Crops Prod. 187, 115386.
Wang, Y., Zhang, X., Chen, J., Chen, A., Wang, L., Guo, X., Niu, Y., Liu, S., Mi, G., Gao, Q., 2019. Reducing basal nitrogen rate to improve maize seedling growth, water and nitrogen use efficiencies under drought stress by optimizing root morphology and distribution. Agric. Water Manag. 212, 328–337.
Xing, H., Zhou, W., Wang, C., Li, L., Li, X., Cui, N., Hao, W., Liu, F., Wang, Y., 2021. Excessive nitrogen application under moderate soil water deficit decreases photosynthesis, respiration, carbon gain and water use efficiency of maize. Plant Physiol. Biochem. 166, 1065–1075.
Ye, T., Ma, J., Zhang, P., Shan, S., Liu, L., Tang, L., Cao, W., Liu, B., Zhu, Y., 2022. Interaction effects of irrigation and nitrogen on the coordination between crop water productivity and nitrogen use efficiency in wheat production on the North China Plain. Agric. Water Manag. 271, 107787.
Yuan, C., Feng, S., Huo, Z., Ji, Q., 2019. Effects of deficit irrigation with saline water on soil water-salt distribution and water use efficiency of maize for seed production in arid Northwest China. Agric. Water Manag. 212, 424–432.
Zhang, G., Hou, Y., Zhang, H., Fan, H., Wen, X., Han, J., Liao, Y., 2022. Optimizing planting pattern and nitrogen application rate improves grain yield and water use efficiency for rain-fed spring maize by promoting root growth and reducing redundant root growth. Soil Tillage Res. 220, 105385.
Zhang, X., Davidson, E.A., Mauzerall, D.L., Searchinger, T.D., Dumas, P., Shen, Y., 2015. Managing nitrogen for sustainable development. Nature 528 (7580), 51–59.